Title

An EMI-Compliant and Automotive-Rated 48V to Point-of-Load Dickson-Based Hybrid Switched-Capacitor DC-DC Converter

ISBN

9798350397420

Authors

Krishnan, Sahana
Blackwell, Margaret E
Pilawa-Podgurski, Robert CN

Publication Date

2023-06-23

DOI

10.1109/itec55900.2023.10187087

2023 IEEE Transportation Electrification Conference & Expo (ITEC), Detroit, MI, USA, June 2023

An EMI-Compliant and Automotive-Rated 48V to Point-of-Load Dickson-Based Hybrid Switched-Capacitor DC-DC Converter

S. Krishnan
M. E. Blackwell
R. C. N. Pilawa-Podgurski

An EMI-Compliant and Automotive-Rated 48V to Point-of-Load Dickson-Based Hybrid Switched-Capacitor DC-DC Converter

Sahana Krishnan, Margaret E. Blackwell, Robert C. N. Pilawa-Podgurski
Department of Electrical Engineering and Computer Sciences
University of California Berkeley

Abstract – With both data center power delivery and automotive powertrains tending towards a 48 V distribution rail, high performance hybrid switched-capacitor (hybrid SC) converters have become an attractive power delivery solution in both spaces. However, automotive power systems present unique challenges in reliability and noise qualifications. This work investigates a regulating Dickson-based hybrid SC topology with low inherent electromagnetic interference (EMI) as well as mitigation techniques, such as an input filter and spread spectrum frequency modulation (SSFM). The proposed filter and modulation schemes enable this converter to meet automotive EMI standards. A hardware prototype combining a power stage and passive input filter is built to demonstrate the merit of hybrid SC topologies for use in 48 V automotive systems.

I. Introduction

Hybrid switched-capacitor (hybrid SC) converters have achieved high efficiency and power density metrics due to their improved utilization of passive components compared to conventional topologies [1]. Particularly, high conversion ratio step-down, 48 V-to-point-of-load (PoL) hybrid SC converters have been recently investigated for use in data centers [2], [3], but these converters are not yet commonly used in the automotive industry due to the more stringent EMI requirements. Though these hybrid SC topologies boast high performance and passive component utilization, they often have a large number of switching elements and, therefore, more switching instances. However, typically, hybrid SC converters have lower switch blocking-voltages and lower dv/dt at the switch nodes, resulting in reduced EMI. This makes them good candidates for use in automotive applications [4].

The similarity in power delivery architecture provides an opportunity to apply the advanced power converter designs used in data center applications to automotive power solutions. Increasing the bus voltage in automotive powertrains from the conventional 12 V bus allows for a reduction in transmission losses as well as reduced cabling weight. In internal combustion engine (ICE) vehicles, 48 V batteries are becoming increasingly popular [5] for partial hybridization of the powertrain to improve efficiency and reduce system weight. Additionally, many electric vehicle (EV) powertrains contain a 48 V "low-voltage" power distribution rail used as an intermediary step-down from the high voltage battery. The power converters themselves must also meet industry EMI requirements so that they can be implemented in the vehicle without interfering with any other electrical subsystems. This work explores two of the most common techniques to mitigate EMI, front-end conducted EMI filter design and Spread-Spectrum Frequency Modulation (SSFM) [6], [7], and analyzes their impacts on size and efficiency of a hybrid SC converter.

This paper presents an 8-to-1 regulating hybrid Dickson switched-capacitor DC-DC power converter with a custom front-end EMI filter to demonstrate the ability of hybrid switched-capacitor converters to meet CISPR 25, Class 5 EMI standards [8], the most stringent class for on-vehicle applications. Section II of the paper details the converter topology and its theory of operation. Section III discusses EMI implications associated with this topology and possible mitigation techniques, most notably front-end filter design and SSFM. Finally, Section IV includes specifications for the experimental prototype and EMI filter as well as measured efficiency and conducted EMI results.

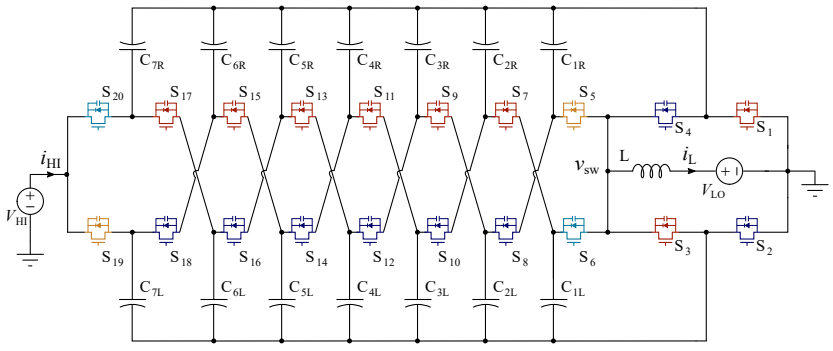

Fig. 1: Schematic drawing of an 8-to-1 interleaved-input Dickson-variant hybrid switched-capacitor converter.

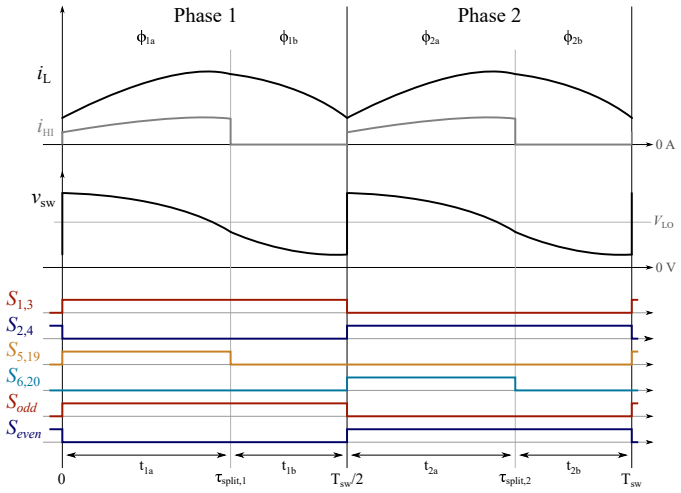

Fig. 2: Exemplar converter waveforms and switching signals for the hybrid Dickson operating at a switching frequency higher than the resonant frequency.

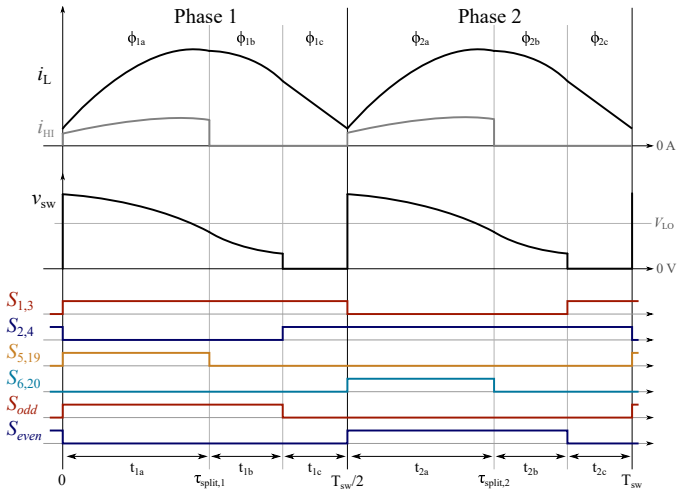

Fig. 3: Switching scheme and exemplar converter waveforms for output voltage regulation of the interleaved-input hybrid Dickson converter operating at a switching frequency faster than resonance.

II. Topology Description

This work utilizes the interleaved-input, single-inductor Dickson topology (Fig. 1) described in [9] to demonstrate efficient, compact, and EMI-compliant DC-DC power conversion in a rugged automotive environment. Even without any additional EMI mitigation, this topology is attractive for automotive off-battery, PoL applications for a number of reasons: interleaved-input, low switch-stress, low dv/dt transitions, and the ability to regulate the output voltage.

In the proposed converter, the interleaved nature of the input allows charge to flow from the high-side source during portions of *both* phases (Fig. 2), rather than just one phase as is typical with many two-phase converters. Because of this quality, the rms value of the input current is reduced as compared to the non-interleaved single-inductor Dickson topology [9], thus, reducing the necessary input capacitance — which is imperative for high power density of the total power conversion system. As described in [1], [10], [11], the family of Dickson-style converters, exemplify minimal total switch stress. Furthermore, the inductor at the low-side port of the converter not only allows for resonant and above-resonant operation, but serves as an output EMI filter, as well as facilitating soft-charging of the flying capacitors [12], [13]. While there are many facets of this topology that make it attractive for both EMI and automotive applications, it does require split-phase operation to maintain soft-charging of the flying capacitors, which is an additional control challenge. Split-phase operation refers to the introduction of two sub-phases within the main switching phases and is discussed more comprehensively in [13].

The resonant frequency of the converter is the switching frequency at which zero-current switching (ZCS) occurs, improving efficiency at light load. However, operating above resonance (i.e., switching faster than resonance) yields better heavy load efficiency where reduced rms currents are achieved in a regime where conduction loss dominates over switching loss. Additionally, operation of hybrid SC converters above resonance provides immunity to component mismatch, which enables the use of high energy density flying capacitors [14], [15]. Tradeoffs of operating this Dickson-variant converter topology at and above resonance are explored in detail in [9], but here, above-resonant operation is necessary to regulate the output voltage as discussed in the following section. The above-resonance switching frequency of the converter prototype is chosen to keep the fundamental switching harmonic below 150 kHz, the lowest end of the EMI regulatory frequency range [8]. Figure 2 shows example inductor current and input current waveforms with corresponding switch gate signals for this converter operating above resonance.

A. Output Voltage Regulation

The topology demonstrated in this work inherently achieves a fixed-conversion ratio. However, due to the output configuration (specifically, output inductor, L, and switches $S_1 - S_4$), this Dickson-variant converter incorporates a merged buck-stage at its output. Therefore, these switches can be controlled to regulate the output voltage to any value lower than the fixed-conversion ratio output. This paper focuses on regulating from the fixed 6 V output voltage down to 5 V. The 5 V bus is an important low voltage rail in an automotive subsystem and supplies downstream loads such as processors, sensors, and in-vehicle networks.

To regulate the output voltage to a level lower than the fixed-ratio output, in this case regulating from 6 V to 5 V, a regulation sub-phase (t_{1c} and t_{2c} in Fig. 3) is inserted within each main switching phase, wherein the output inductor is shorted to ground [15], [16]. Phase 1 consists of Phase 1a (Fig. 4a), its corresponding split-phase, Phase 1b (Fig. 4b), and its regulating sub-phase, Phase 1c (Fig. 4c). Similarly, Phase 2 consists of Phase 2a (Fig. 4d), Phase 2b (Fig. 4e), and Phase 2c (Fig. 4f). During the regulating intervals, switches $S_5 - S_{20}$ are off and the current through inductor L freewheels via the four bridge switches, $S_1 - S_4$. The duration of each regulation sub-phase is set according to the required output voltage and the relationship between the switching frequency and resonant frequency.

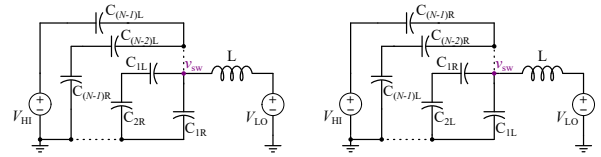

(a) Phase 1a. (d) Phase 2a.

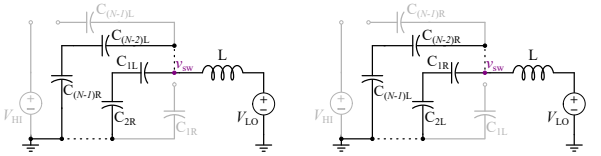

(b) Phase 1b. (e) Phase 2b.

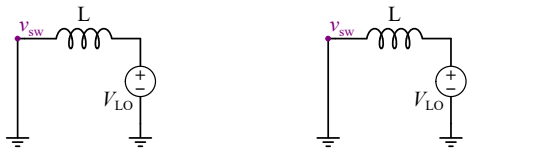

(c) Phase 1c. (f) Phase 2c.

Fig. 4: Equivalent circuits for each sub-phase of a regulating 8-to-1 Dickson converter, with split-phase switching and regulating sequence as ordered a-f: Phase 1a → Phase 1b → Phase 1c → Phase 2a → Phase 2b → Phase 2c.

III. EMI Mitigation Techniques

Automotive power converters are generally placed in close proximity to other in-vehicle electronics, many of which are susceptible to EMI. Thus, the high di/dt and dv/dt associated with the power converter switching transitions (made steeper by the implementation of high-speed, wide-bandgap power transistors such as GaN) must be mitigated [17], [18]. In automotive systems, the allowable EMI noise levels are standardized in CISPR 25, with Class 5 limit requirements [8]. The EMI spectrum is measured over the frequency range of 150 kHz to 108 MHz and there are peak, quasi-peak and average, noise limits set within this range. A summary of the specifications for this standard are presented in Table I. Full compliance testing requires peak, quasi-peak and average detectors, however, both the quasi-peak and average data will not exceed the peak levels [19]. In this paper, peak EMI data is reported to understand "worst case" noise levels for the converter, and average data is reported to more clearly demonstrate the positive impact of SSFM on noise levels.

This work focuses on reducing the conducted emissions of

TABLE I: Conducted Noise Limits for CISPR 25, Class 5 EMI Standards [8]

Band	Frequency (MHz)	Limit (dBμV)	
		Peak	Average
LW	0.15-0.3	70	50
MW	0.53-1.8	54	34
SW	5.9-6.2	53	33
FM	76-108	38	18
TV	41-88	34	24
CB	26-28	44	24
VHF I	30-54	44	24
VHF II	68-87	38	18

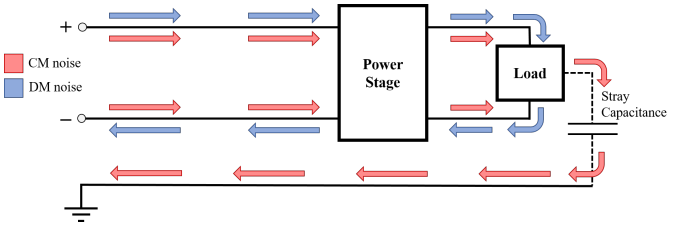

Fig. 5: Common Mode and Differential Mode noise paths through the system.

the converter — in this case, measured in a pre-compliance setup, which provides a good indication of overall EMI performance. Noise from conducted emissions can be broken down into two different types: common mode (CM) and differential mode (DM), shown in Fig. 5. CM refers to noise in which the direction of the "noise currents" on the positive and negative lines of the power converter have the same direction. For DM noise, the "noise current" flows in the same direction as the power converter current. CM noise is increased by parasitic capacitance in the power stage and the switched output voltage [7], [20], [21]. On the other hand, DM noise is worsened by increasing current through the converter. Higher load current will exacerbate the impact of parasitics in larger current loops throughout the power stage [7]. For applications which utilize a distribution bus, such as the 48 V bus in automotive power trains, it is crucial to shield the bus from noise generated by switching converters. Therefore, here, we are primarily interested in the CM and DM noise as seen by the high-side (or 48 V input) source.

There are several ways to reduce conducted EMI in switching power converters. EMI filters are a common addition to the front-end of a power stage and can be tuned to mitigate problematic noise peaks within the EMI measurement range. Additionally, spread spectrum frequency modulation (SSFM) is a well-known control technique that involves using a variable switching frequency to spread the noise peaks across a range of frequencies to reduce conducted EMI [6]. Different SSFM schemes and their specific impacts on converter EMI are explored in more detail in [9]. In this work, a passive front-end EMI filter is designed to reduce noise at specific frequencies. In conjunction with the filter, a trapezoidal SSFM scheme is implemented to further spread out the noise peaks and reduce filter sizing.

A. Passive Front-End EMI Filter

A passive component filter at the high-side of the power stage is designed to target CM and DM noise at specific frequencies. A discrete front-end filter is only added to the hybrid SC converter at the high-side port due to the inherent filtering inductor of the hybrid SC converter at the low-side port.

The EMI filter circuit design in this work is depicted in Fig. 6. In general, a damping network may be needed in case of significant peaking at the filter corner frequency, however, for this converter, the additional damping was not necessary. The filter components are chosen based on preliminary conducted

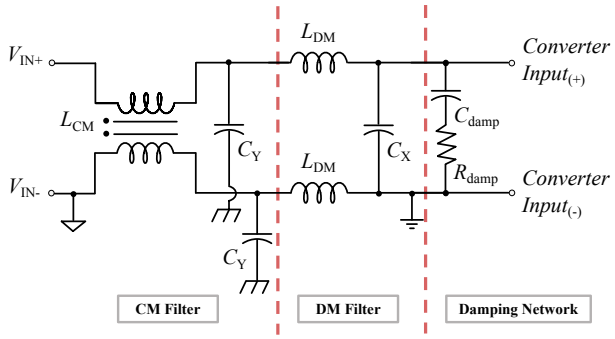

Fig. 6: Schematic of the front-end EMI filter.

EMI measurements of the converter. The EMI performance without filtering is used to determine at which specific frequencies the noise peaks occur. Then, this noise is targeted with the filter design. For this 48-to-5 V Dickson converter operating at 106 kHz, the noise peaks that need to be filtered to meet the CISPR 25 occur at harmonics of the converter switching frequency. In the CM case, the peaks occur at the second and fourth harmonics of the converter switching frequency, which also correspond to the fundamental and second harmonic of the switched input current frequency. In the DM case, they occur at the second, fourth, and sixth switching harmonics (i.e., the first, second, and third harmonic of the input current). The required attenuation between the noise peak and the EMI standard limit, termed insertion loss (IL) [22], is determined for both CM and DM noise, and this parameter is used to design the EMI filter components.

Based on the initial EMI measurements at the operating conditions of interest, standardized discrete component values for the CM and DM filter are chosen. EMI attenuation in practice can deviate from the calculated value due to factors such as parasitic elements and impedance mismatch [23]. Therefore, an iterative process is required to tune the filter according to measured EMI results.

B. Spread-Spectrum Frequency Modulation (SSFM)

Because EMI filters add to overall passive component volume and loss, spread spectrum, or "dithering", frequency techniques can also be used to further reduce conducted EMI that is generated by fixed-frequency switching schemes. This dithering technique can spread out and lower the original noise peaks at the switching harmonics. There are a variety of periodic and random SSFM methods that can be used to achieve this goal [6], [24], and a trapezoidal modulation scheme is implemented in this paper. In the trapezoidal modulation method, the switching frequency is varied higher and lower about the original center frequency by a trapezoidal modulation carrier.

The trapezoidal modulation scheme has similar advantages and disadvantages as triangular modulation, which is detailed in [9], [24]. Ramping the switching frequency up and down avoids noise spiking at any specific frequency and its harmonics [6]. Trapezoidal SSFM also evenly spreads the energy away from the center frequency, creating a mostly flat energy band which helps to lower noise peaks. Since the switching frequency is being manipulated periodically, one drawback of this method is that both the input and output voltages can acquire a periodic ripple at the modulation frequency. Therefore, the modulation frequency should be chosen to be sufficiently slow to avoid too much overlap with the fundamental frequency and its harmonics. For the implementation in this work, the dithering step size is $\pm$ 0.5 kHz with a maximum deviation of $\pm$ 3.5 kHz from the center frequency at a modulation frequency of 700 Hz.

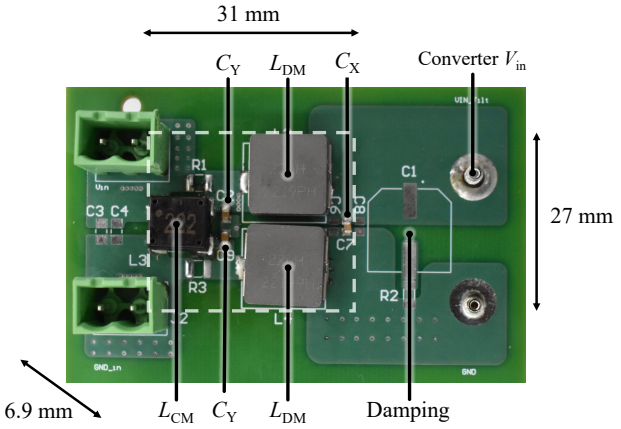

Fig. 7: Photograph of EMI filter daughter board.

IV. Experimental Prototype

An 8-to-1 discrete hardware prototype of an interleaved-input Dickson variant hybrid SC was built to demonstrate high efficiency, power density, and EMI compliance [9]. Annotated photographs of the front-end filter and full converter are shown in Figs. 7 and 8. This prototype uses only automotive-qualified components to ensure adherence to the Automotive Electronics Council (AEC) standard. The converter flying capacitors (C_{R1-7} and C_{L1-7}) and inductor (L) values were chosen to give an effective resonant switching frequency of 42 kHz. This resonant switching frequency was chosen such that twice the resonant frequency is less than the lowest frequency of the EMI measurement range, 150 kHz.

A. Operation

Both inductor current, i_L, and switch-node voltage, v_{sw}, waveforms are shown in Fig. 9 for resonant, above resonant, and regulating operation of the hardware prototype at the

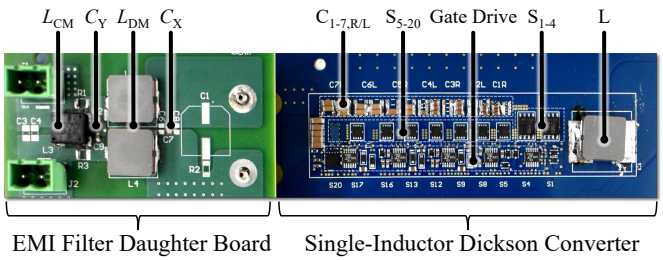

Fig. 8: Photograph of EMI filter daughter board mounted on power stage prototype. Power stage components are mirrored on the top and bottom side of the PCB.

TABLE III: Component Listing of the EMI Filter

Component	Mfr. & Part Number	Parameters
Common Mode (CM) Filter		
CM Choke, L_{CM}	Würth Elektronik 744273222	30 μH, 1.4 A I_{sat}
CM "Y" Capacitance, C_{Y}	TDK CGA6M2X7R2A474M200AA	X7R, 100 V, 0.47 μF
Differential Mode (DM) Filter		
DM Inductors, L_{DM}	Vishay Dale IHLP5050EZER220M5A	22 μH, 6.9 A I_{sat}
DM "X" Capacitance, C_{X}	Kemet C0805C224K5RACAUTO	50 V, 0.22 μF

TABLE II: Converter Operating Parameters

Parameter	Value	Units
V_{HI}	48	V
V_{LO}	5, 6	V
$P_{\text{LO},max}$	120	W
f_{sw}	106	kHz
f_{res}	42	kHz
L	0.64	μH
C^*_{in}	60	μH
C^*_{fly}	6	μH

* Voltage-de-rated values.

conditions listed in Table II. Operating above resonance comes with reduced rms currents compared to resonant operation. This is beneficial when the converter needs to be pushed to higher load currents, a regime where conduction loss dominates [9]. The regulating case has higher rms currents compared to operating above resonance at a fixed conversion ratio, incurring more conduction losses in the switches and magnetics. Furthermore, switches $S_1 - S_4$ conduct for a longer amount of time (depicted in Fig. 3), again resulting in increased losses. Higher di/dt transitions in the regulating case also contribute to higher core loss in the inductor [16].

Fig. 10 shows efficiency versus load curves measured for regulating and unregulating variants of the converter, both with and without the EMI filter when the converter is operated at a switching frequency of ∼106 kHz (2.5× above the resonant frequency). The peak efficiency of the unregulated converter ($V_{LO} \sim 6$ V) with EMI filter is 97.3% at a load of 5 A whereas, the peak efficiency at $V_{\text{LO}} = 5$ V is 94.7%, including the EMI filter.

B. Implementation of EMI Mitigation Techniques

An EMI filter daughter board was designed, built, and connected at the input side of the power stage prototype board. Fig. 7 depicts the EMI filter board with Fig. 8 showing the filter daughter board size in comparison to the power stage. The EMI filter measures 31 mm × 27 mm × 7 mm and accounts for 21% of the overall converter volume. The passive components for both the CM and DM filter are listed in Table II.

Preliminary EMI noise levels, for the converter operating at 2.5× the resonant switching frequency with no EMI filter

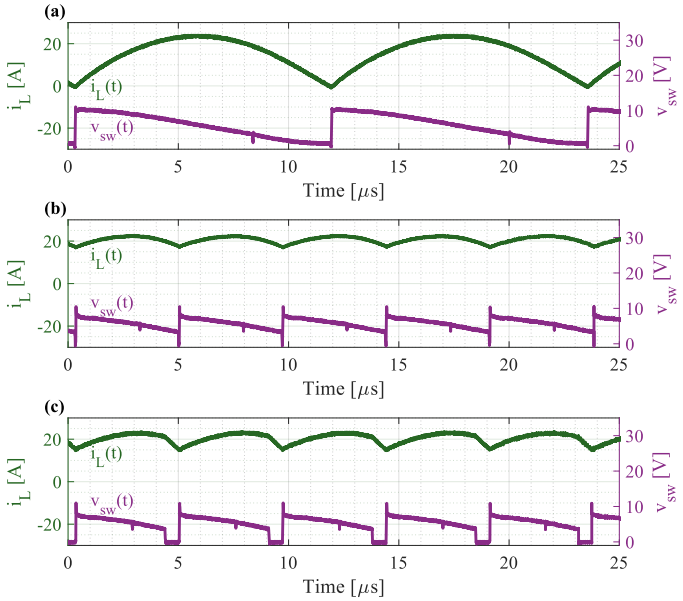

Fig. 9: (a) Resonant, (b) above resonant, and (c) regulating inductor current, i_L, and switch-node voltage, v_{sw}, measured waveforms for the 8-to-1 discrete hardware prototype.

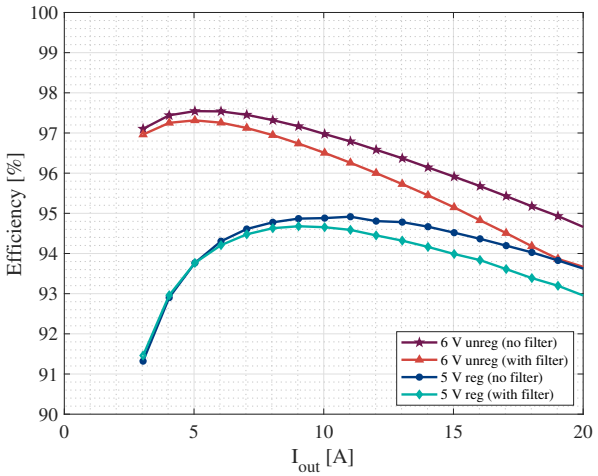

Fig. 10: Measured efficiency of 8-to-1 hardware prototype at 48 V input and both nominal 6 V output and regulated 5 V output, switching at 106 kHz (2.5× faster than resonance).

are shown in Fig. 11. These initial measurements inform the EMI filter design. The highest noise peaks within the CISPR frequency range — which the filter targets — occur at the second switching harmonics for both CM and DM noise. Applying the designed CM filter with corner frequency 42 kHz

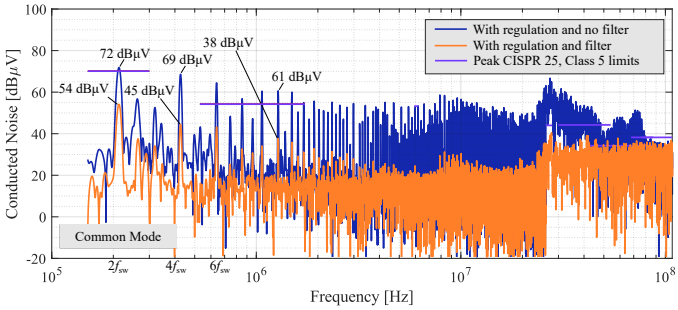

(a) Peak common mode (CM) conducted emissions.

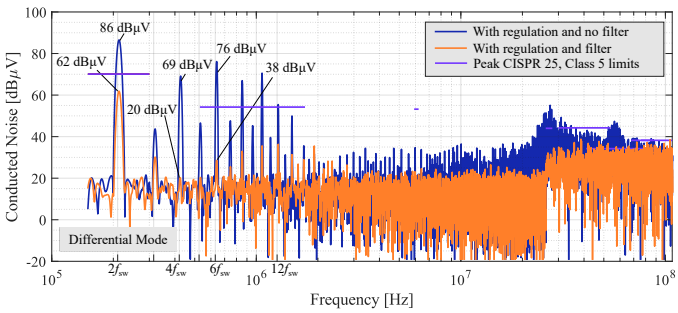

(b) Peak differential mode (DM) conducted emissions.

Fig. 11: Peak CM and DM emissions plots for above-resonant (∼106 kHz) regulating operation with and without EMI filter (22 μH DM inductors) and no SSFM.

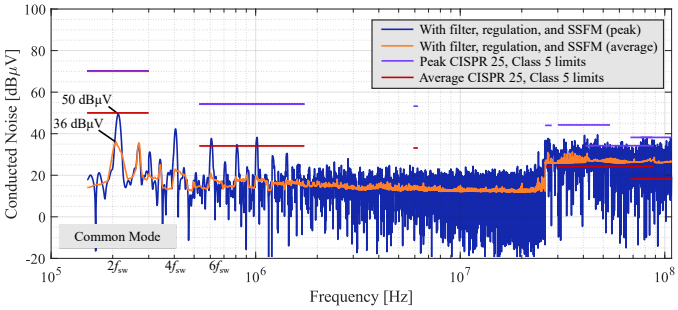

(a) Peak and average common mode (CM) conducted emissions.

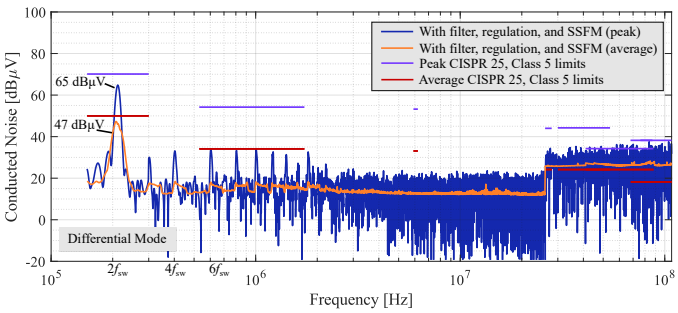

(b) Peak and average differential mode (DM) conducted emissions.

Fig. 12: Peak and average CM and DM emissions plots for above-resonant (∼106 kHz) regulating operation with reduced filter size (15 μH DM inductors) and SSFM enabled.

and the DM filter at 72 kHz, the noise peaks for CM and DM conducted emissions are reduced by more than 85%, as seen in Figs. 11a and 11b. The 48 V converter with passive EMI filter now passes CISPR 25, Class 5 limits. The high frequency noise between 26 MHz and 108 MHz does not come from the power stage itself. This noise is a measured phenomenon of the pre-compliant setup which contains both an electronic power supply and load and which is not fully enclosed.

Where passive component volume is a primary concern, SSFM can be employed in lieu of or in conjunction with an EMI filter, depending on the noise levels that must be mitigated. The impacts of a trapezoidal SSFM scheme on conducted EMI are demonstrated in Fig. 12. The key observation is that when SSFM is implemented, both the CM and DM noise peaks are lower and more spread out. This enables optimization of the EMI filter size, and the DM filter inductance is decreased from the initial 22 μH calculated value to 15 μH – a reduction of over 30%. With SSFM, the fundamental switching frequency is changing periodically, so the noise peaks will occur at different harmonics along the EMI measurement range at the time of the measurement. In this case, an average EMI measurement is useful to showcase the true impact of SSFM. Average detection takes the average amplitude of each noise signal across its period. As shown in Fig. 12, the converter with passive EMI filter and SSFM passes both peak and average CISPR 25, Class 5 limits when focusing on the lower frequency bands and disregarding the high-frequency noise due to the pre-compliant setup.

V. Conclusion

The development of a 48 V distribution bus in both EVs and ICE vehicles opens opportunities for adapting advancements in high-efficiency, high-power-density data center power conversion techniques to automotive applications. However, power electronics in vehicles require robust component selection and qualification for industry EMI standards. This paper discusses the construction of an automotive EMI pre-qualified regulating 8-to-1 hybrid Dickson switched-capacitor converter for 48 V-to-PoL conversion. EMI mitigation techniques are discussed in detail, particularly regarding their implementations in hybrid SC converters. Conducted EMI results showcasing the benefits of the input filter and SSFM implementation are reported demonstrating the interleaved-input hybrid Dickson converter passing CISPR 25, Class 5 EMI specifications.

References

[1] Z. Ye, S. Sanders, and R. C. N. Pilawa-Podgurski, "Modeling and Comparison of Passive Component Volume of Hybrid Resonant Switched-Capacitor Converters," *IEEE Transactions on Power Electronics*, 2022.

[2] Y. Li, X. Lyu, D. Cao, S. Jiang, and C. Nan, "A 98.55% Efficiency Switched-Tank Converter for Data Center Application," *IEEE Transactions on Industry Applications*, vol. 54, no. 6, pp. 6205–6222, 2018.

[3] J. Baek, P. Wang, S. Jiang, and M. Chen, "LEGO-PoL: A 93.1% 54V-1.5V 300A Merged-Two-Stage Hybrid Converter with a Linear Extendable Group Operated Point-of-Load (LEGO-PoL) Architecture," in *2019 20th Workshop on Control and Modeling for Power Electronics (COMPEL)*, 2019, pp. 1–8.

[4] J. W. Kwak and D. B. Ma, "An Automotive-Use Dual-fsw-Zone Hybrid Switching Power Converter with Vo-Jitter-Immune Spread-Spectrum Modulation," in *ESSCIRC 2022- IEEE 48th European Solid State Circuits Conference (ESSCIRC)*, 2022, pp. 281–284.

[5] J. Bilo *et al.*, "48-Volt Electrical Systems – A Key Technology Paving the Road to Electric Mobility," ZVEI-German Electrical and Electronic Manufacturers' Association Electronic Components and Systems and PCB and Electronic Systems Divisions, Apr 2016. [Online].

[6] D. Gonzalez, J. Balcells, A. Santolaria, J.-C. Le Bunetel, J. Gago, D. Magnon, and S. Brehaut, "Conducted EMI Reduction in Power Converters by Means of Periodic Switching Frequency Modulation," *IEEE Transactions on Power Electronics*, vol. 22, no. 6, pp. 2271–2281, 2007.

[7] K. Mainali and R. Oruganti, "Conducted EMI Mitigation Techniques for Switch-Mode Power Converters: A Survey," *IEEE Transactions on Power Electronics*, vol. 25, no. 9, pp. 2344 – 2356, 2010.

[8] International Electrotechnical Commission (IEC), "CISPR 25 Vehicles, Boats and Internal Combustion Engines – Radio Disturbance Characteristics – Limits and Methods of Measurement for the Protection of On-Board Receivers," October 2016.

[9] M. E. Blackwell, S. Krishnan, N. M. Ellis, and R. C. Pilawa-Podgurski, "Direct 48 V to 6 V Automotive Hybrid Switched-Capacitor Converter with Reduced Conducted EMI," in *2022 IEEE 23rd Workshop on Control and Modeling for Power Electronics (COMPEL)*, 2022, pp. 1–8.

[10] M. H. Kiani and J. T. Stauth, "Optimization and Comparison of Hybrid-Resonant Switched Capacitor DC-DC Converter Topologies," in *2017 IEEE 18th Workshop on Control and Modeling for Power Electronics (COMPEL)*. IEEE, 2017, pp. 1–8.

[11] P. H. McLaughlin, J. S. Rentmeister, M. H. Kiani, and J. T. Stauth, "Analysis and Comparison of Hybrid-Resonant Switched-Capacitor DC–DC Converters With Passive Component Size Constraints," *IEEE Transactions on Power Electronics*, vol. 36, no. 3, pp. 3111–3125, March 2021.

[12] R. C. Pilawa-Podgurski and D. J. Perreault, "Merged Two-Stage Power Converter With Soft Charging Switched-Capacitor Stage in 180 nm CMOS," *IEEE Journal of Solid-State Circuits*, vol. 47, no. 7, pp. 1557–1567, 2012.

[13] Y. Lei, R. May, and R. Pilawa-Podgurski, "Split-Phase Control: Achieving Complete Soft-Charging Operation of a Dickson Switched-Capacitor Converter," *IEEE Transactions on Power Electronics*, vol. 31, no. 1, pp. 770–782, 2016.

[14] M. D. Seeman and S. R. Sanders, "Analysis and Optimization of Switched-Capacitor DC–DC Converters," *IEEE Transactions on Power Electronics*, vol. 23, no. 2, pp. 841–851, March 2008. [Online]. Available: http://ieeexplore.ieee.org/document/4463867/

[15] C. Schaef, J. Rentmeister, and J. T. Stauth, "Multimode Operation of Resonant and Hybrid Switched-Capacitor Topologies," *IEEE Transactions on Power Electronics*, vol. 33, no. 12, pp. 10 512–10 523, Dec 2018.

[16] P. S. Shenoy, M. Amaro, J. Morroni, and D. Freeman, "Comparison of a Buck Converter and a Series Capacitor Buck Converter for High-Frequency, High-Conversion-Ratio Voltage Regulators," *IEEE Transactions on Power Electronics*, vol. 31, no. 10, pp. 7006 – 7015, 2015.

[17] D. Han, S. Li, W. Lee, W. Choi, and B. Sarlioglu, "Trade-off Between Switching Loss and Common Mode EMI Generation of GaN Devices-Analysis and Solution," in *2017 IEEE Applied Power Electronics Conference and Exposition (APEC)*, 2017, pp. 843–847.

[18] L. Middelstaedt, B. Strauss, and A. Chupryn, "Investigation of the Root Causes of Electromagnetic Noise of an Interleaved DC–DC Converter With GaN or Si Transistors and Corresponding Optimization Strategies," *IEEE Journal of Emerging and Selected Topics in Power Electronics*, vol. 8, no. 8, pp. 2759 – 2774, 2020.

[19] R. Martinez and Z. Zhang, "Fundamentals of EMI Requirements for an Isolated DC/DC Converters," 2021. [Online].

[20] N. Mutoh, M. Nakanishi, M. Kanesaki, and J. Nakashima, "EMI Noise Control Methods Suitable for Electric Vehicle Drive Systems," *IEEE Transactions on Electromagnetic Compatibility*, vol. 47, no. 4, pp. 930–937, 2005.

[21] Y. H. Lee and A. Nasiri, "Conductive CM and DM Noise Analysis of Power Electronic Converters in Electric and Hybrid Electric Vehicles," in *2007 IEEE Vehicle Power and Propulsion Conference*, 2007, pp. 1–6.

[22] B. Audone and L. Bolla, "Insertion Loss of Mismatched EMI Suppressors," *IEEE Transactions on Electromagnetic Compatibility*, vol. EMC-20, no. 3, pp. 384–389, 1978.

[23] F. Luo, D. Boroyevich, P. Mattavelli, and H. Bishnoi, "EMI Filter Design Considering In-Circuit Impedance Mismatching," in *2012 IEEE Energy Conversion Congress and Exposition (ECCE)*, 2012, pp. 4613–4618.

[24] S. Jaffe, "The Pros and Cons of Spread-Spectrum Implementation Methods in Buck Regulators," 2021. [Online].